Quantum Electronics **50** (6) 608–612 (2020)

NANOPHOTONICS https://doi.org/10.1070/QEL17218

Spectral features of colloidal solutions of elongated gold nanoparticles produced by laser ablation in aqueous solutions

M.I. Zhil'nikova, G.A. Shafeev, E.V. Barmina, Yu.L. Kalachev, O.V. Uvarov

Abstract. **The extinction spectra of colloidal solutions of gold nanoparticles produced by laser ablation in water and aqueous solutions of salts using two near-IR lasers with pulse durations of 200 ns and 1 ps are experimentally investigated. The extinction spectrum of the particles formed by ablation in aqueous solutions is characterised by enhanced optical density in the red and IR regions. This feature is due to the formation of elongated gold nanoparticles, as confirmed by transmission electron microscopy. The surface images of a gold target subjected to multipulse laser ablation exhibit micron and submicron structures.**

Keywords: *laser ablation, liquid, gold nanoparticles.*

1. Introduction

Gold nanoparticles are of great interest for many researchers because of the specificity of their physicochemical properties [1]. One of the most popular techniques for fabricating such particles is laser ablation in liquids [2–6]. Various processes accompanying laser impact on gold targets were investigated in a number of studies [7–11].

The formation of nanoparticles is the result of the interaction of laser radiation with target and subsequent removal of target material particles from the target surface, forced by the pressure of vapor of the liquid surrounding the target. The processes of generation of gold nanoparticles and their optical properties were investigated in [12–14]. Individual nanoparticles produced during laser ablation in a liquid may interact with laser radiation in the liquid, due to which their morphology and size distribution function change. Ablation is accompanied by plasma formation near the target surface and around nanoparticles, as well as generation of hydrogen, oxygen, and hydrogen peroxide [15–17].

M.I. Zhil'nikova Prokhorov General Physics Institute, Russian Academy of Sciences, ul. Vavilova 38, 119991 Moscow, Russia; Moscow Institute of Physics and Technology (National Research University), Institutskii per. 9, 141701 Dolgoprudnyi, Moscow region, Russia; e-mail: margarita.zhilnikova@phystech.edu;
G.A. Shafeev Prokhorov General Physics Institute, Russian Academy of Sciences, ul. Vavilova 38, 119991 Moscow, Russia; National Research Nuclear University MEPhI (Moscow Engineering Physics Institute), Kashirskoe shosse 31, 115409 Moscow, Russia;
E.V. Barmina, Yu.L. Kalachev, O.V. Uvarov Prokhorov General Physics Institute, Russian Academy of Sciences, ul. Vavilova 38, 119991 Moscow, Russia

Received 6 December 2019; revision received 12 February 2020
Kvantovaya Elektronika **50** (6) 608–612 (2020)
Translated by Yu.P. Sin'kov

Previously we investigated elongated gold nanoparticles obtained by laser ablation in water [18]. The radiation source was an ytterbium-doped fibre laser with a pulse duration of 200 ns. It was found that the presence of Ca^{2+} ions in water (as a result of dissociation of $CaCl_2$ salt) leads to the formation of nanoparticle chains. It was also revealed that nanoparticles agglomerate into chains up to 1 μm long in the early irradiation stage. The interaction of laser radiation with aqueous colloids of elongated nanoparticles as function of the pulse energy and irradiation time was analysed. It was found that nanoparticle agglomeration is replaced with fragmentation under long-term laser impact on an initial colloidal solution. Our next study [19] was devoted to similar processes occurring as a result of introduction of other divalent ions [admixtures in the form of salts $BaSO_4$, $MgSO_4$, and $Be(NO_3)_2$] into water. A specific feature of nonspherical particles is known to be the presence of two plasmon resonances, longitudinal and transverse, whose positions depend on the particle length-to-diameter ratio (aspect ratio). The longitudinal resonance in elongated nanoparticles is red-shifted. The extinction spectra of colloidal solutions of gold nanoparticles obtained by ablation in the presence of divalent ions exhibit a pronounced shift of maximum absorption (corresponding to the position of transverse plasmon resonance) with an increase in concentration; in addition, a wing arises in the IR region, thus confirming the elongated shape of nanoparticles. Since gold is diamagnetic, gold particles exhibit diamagnetic behaviour. However, elongated nanoparticles can be affected by an external magnetic field under certain conditions. For example, an exposure of these nanoparticles to a 7-T magnetic field for several tens of minutes leads to their further elongation and formation of nanorods with an aspect ratio up to 17–18 [20].

In this paper, we report the results of studying and comparing the extinction spectra of colloidal solutions and the morphology of gold nanoparticles fabricated using 200-ns and 1-ps laser pulses, as well as nanoparticles obtained with different divalent ions introduced into solution. In addition, the influence of the laser ablation duration and concentration of divalent ions on the spectra and morphology of nanoparticles was investigated.

2. Experimental

Gold nanoparticles were fabricated by laser ablation of a solid target immersed in liquid. The radiation sources were as follows: a pulsed ytterbium-doped fibre laser with a wavelength of 1060–1070 nm and a 1060-nm laser based on ytterbium-doped potassium–gadolinium tungstate crystal (Yb:KGW).

The radiation of both lasers was linearly polarised. The pulse duration and repetition rate were, respectively, 200 ns and 20 kHz for the fibre laser and 1 ps and 1 kHz for the Yb:KGW laser. Nanoparticles were fabricated as a result of ablation of an Au target in Milli-Q water (volume of 12 mL). The target was a gold plate with a purity of 99.9%. A laser beam focused on the target surface (with a spot diameter in the focal plane of ~50 μm for the fibre laser and 30 μm for the Yb:KGW laser) was horizontally displaced using a LaserScan system with an F-Theta objective. The electric drive of the system made it possible to move the beam over the target surface with a velocity of 500 mm s^{-1}. The liquid layer thickness above the target was 2–3 mm. In each series of experiments gold nanoparticles were generated for 1 min in the case of fibre laser and for 20 min (on average) in the case of Yb:KGW laser.

Spectral analysis of the prepared colloidal solutions was performed using an Ocean Optics USB-LS-450 fibre spectrometer (in the visible region) and Shimadzu-3600 and Cary spectrometers (in the IR region). The laser fluence was calculated from the radiation power, pulse repetition rate, and laser spot area. The sizes of the laser spot on the target surface were determined as the sizes of irradiated area (measured with an optical microscope).

The nanoparticle morphology was investigated with a transmission electron microscope (TEM), and the gold target surface was studied using a scanning electron microscope (SEM) and energy-dispersive analysis (EDX).

3. Results

In the first series of experiments we studied the interaction of laser radiation with solid gold target in water. First, the radiation source was an ytterbium-doped fibre laser with a pulse duration of 200 ns. The irradiation time was 1 min; the average radiation powers were 9.7, 13.0, and 16.2 W; and the fluences were 12.2, 13.7, and 13.0 J cm^{-2}, respectively. We could not observe any direct relationship between the aforementioned values with an increase in the average power, which is due to the difference in the laser spot diameter at different radiation powers. The ablation threshold was 8.32 J cm^{-2}. The extinction spectra of colloidal solutions of gold nanoparticles are presented in Fig. 1. These spectra, as well as the ones presented in other figures, are normalised to the optical density at λ = 377 nm. The reason is that the imaginary part of permittivity of spherical gold nanoclusters at a given wavelength is independent of their sizes and morphology [21]. It should also be noted that the position of the only absorption peak (corresponding to the transverse plasmon resonance [22]) is independent of the fluence, and the peak is located near λ = 523 nm. At the same time, no absorption peaks were observed in the IR region.

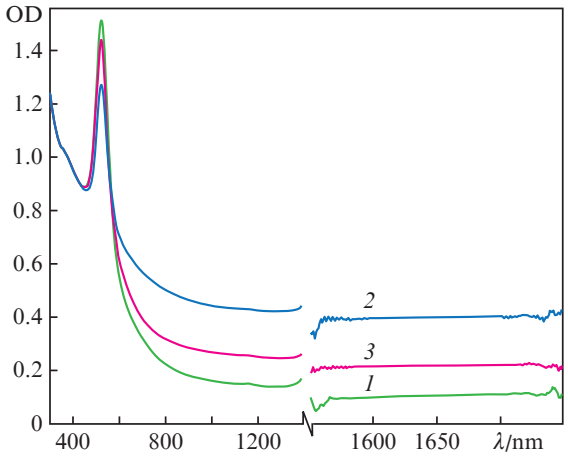

Figure 1. Extinction spectra (optical density OD) of colloidal solutions of gold nanoparticles in water, obtained by ablation of a target using ytterbium laser radiation with fluences of (*1*) 12.2, (*2*) 13, and (*3*) 13.7 J cm^{-2}. The break in the wavelength axis is due to the presence of strong absorption line of H_2O molecules at $\lambda \approx$ 1400 nm.

Figure 2 shows extinction spectra of the colloidal solutions of gold nanoparticles obtained as a result of ablation of a target in water and aqueous solutions using an ytterbium-doped fibre laser. It can be seen that, in the case of ablation in pure water, the spectrum of nanoparticles has an absorption peak typical of spherical gold nanoparticles in water (near 523 nm), while introduction of a small amount of calcium chloride (concentration of 0.8 mg L^{-1}) into the ablation medium leads to the formation of particles with another spectrum, which is related to a change in their morphology. There are additional absorption peaks in the near-IR region, between 600 and 1200 nm, as well as between 1670 and 1750 nm. This influence of the medium on the spectra of nanoparticle solutions was described in detail in [19]. The existence of these peaks in spectra suggests the presence of elongated particles in the solution, which are characterised by various longitudinal resonances. Thus, the presence of divalent ions in water leads to the formation of nanoparticles with unique morphology during laser ablation.

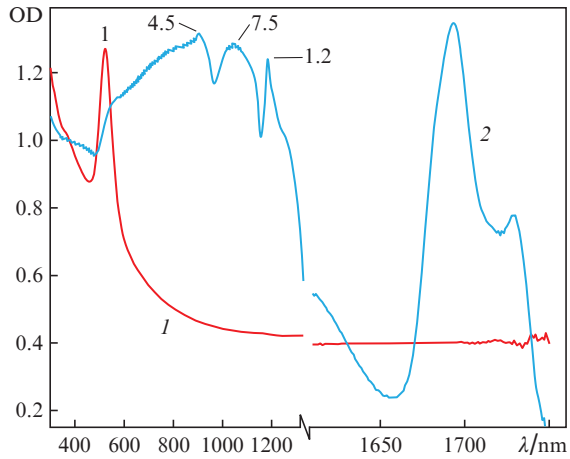

Figure 2. Extinction spectra of colloidal solutions of gold nanoparticles obtained by ablation of a target (using ytterbium laser radiation) in (*1*) water and (*2*) water with an admixture of $CaCl_2$ (concentration 0.8 mg L^{-1}). The numbers at peaks are the aspect ratios of the particles corresponding to them.

Note that the salts dissolved in water have not any absorption bands in the visible and IR spectral regions.

To obtain colloidal solutions of nanoparticles in large volumes, the target surface should be subjected to multipulse (10^8–10^9 pulses) laser irradiation. As a result, the target surface becomes uneven. The SEM images of the gold target surface demonstrate that it is coated by characteristic spherical structures of micron and submicron sizes (Fig. 3). There are many microspheres with sizes on the order of several micrometers. The EDX data confirm that the microspheres

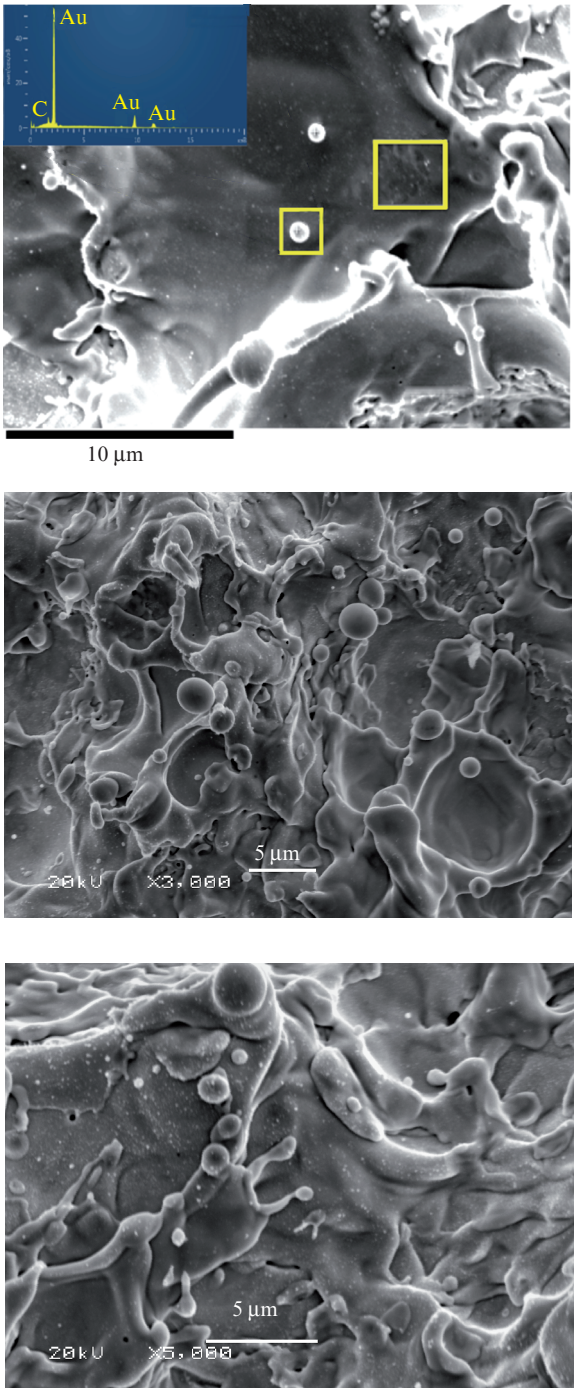

Figure 3. SEM images of a gold target surface subjected to laser ablation, taken at angles of (a) 0 and (b, c) 20°. The inset in Fig. 3a presents the EDX data (X-ray spectrum) on two isolated areas of the target surface, one of which contains a microsphere. The microsphere elemental composition is identical to that of the entire surface (a).

consist of gold, as well as the target surface nearby, independent of the concentration of divalent ions in the solution. It should also be added that the particles of this size do not contribute to the plasmon resonance (because the latter is absent), although the fraction of ablated material is rather large. Therefore, there are no additional peaks in the spectrum. Based on the obtained images, one can conclude that the absorptivity of such surfaces greatly exceeds that of flat ones. In addition, one can see many solidified spikes on the target surface, which indicate loss of the target material due to the development of hydrodynamic instabilities at the interface between the melt and vapour bubble.

In the second series of experiments magnesium sulfate (concentration of 5 mg L^{-1}) was added to water as a source of divalent ions. The target irradiation time was varied. It can be seen in Fig. 4 that an increase in the ablation time affects the nanoparticle elongation. This follows from the enhancement of absorption in the red spectral region. It is noteworthy that long-term ablation (up to 40 min) shifts the position of the maximum of plasmon resonance from 521 to 534 nm, which is another evidence of a change in the particle morphology. The occurrence of a wide wing in the spectrum is due to the superposition of longitudinal resonance peaks for nanoparticles with different aspect ratios [23, 24]. The normalisation of spectra to the optical density value at λ = 377 nm suggests the following: the number of elongated particles increases with an increase in the irradiation time, as is evidenced by the increase in the area under each individual spectrum. Under these conditions, the amplitude of the transverse-resonance absorption peak barely increases, which indicates conservation of the number of spherical particles in the colloid.

The magnesium sulfate concentration in water was varied from 0 to 80 mg L^{-1} in the experiments described below; the ablation time was 5 min. It can be seen in Fig. 5 that, for the

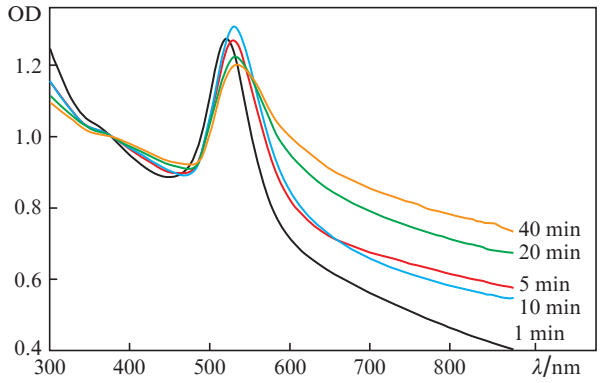

Figure 4. (Colour online) Extinction spectra of colloidal solutions of gold nanoparticles obtained by laser ablation in water with an admixture of $MgSO_4$ (concentration 5 mg L^{-1}); the ablation time is 1–40 min.

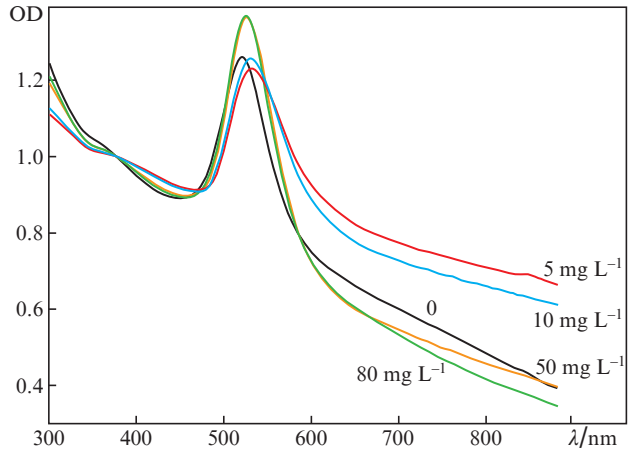

Figure 5. (Colour online) Extinction spectra of colloidal solutions of gold nanoparticles obtained by laser ablation in an $MgSO_4$ aqueous solution (concentration 0–80 mg L^{-1}); the ablation time is 5 min.

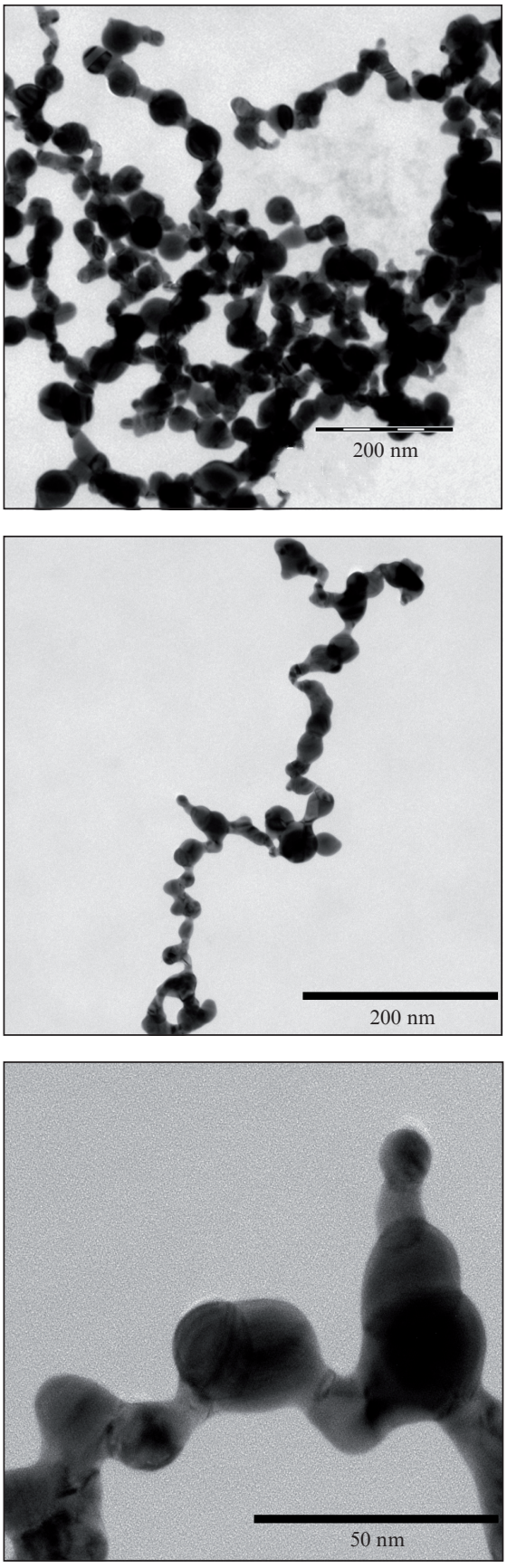

Figure 6. TEM images of a colloidal solution of gold nanoparticles produced by laser ablation in water with an admixture of $MgSO_4$ salt (concentration 5 mg L^{-1}): (a) general view, (b) individual particle, and (c) fragment of individual particle; the ablation time is 5 min.

concentrations of 5 and 10 mg L^{-1}, the optical density in the range of 600–900 nm exceeds that for other concentrations. It should be noted that the presence of magnesium cannot be revealed by EDX (within the measurement sensitivity) at these concentrations.

Figure 6 shows TEM images of gold nanoparticles obtained by ablation of a gold target in water with $MgSO_4$ salt added. It can be seen that the particle length may exceed 400 nm.

Figure 7 shows the extinction spectra of an aqueous solution of gold nanoparticles obtained by ablation using an Yb:KGW laser with a pulse duration of 1 ps. The following feature is noteworthy: when the magnesium sulfate concentration reaches 5 mg L^{-1}, the IR wing is absent in the extinction spectrum, whereas in the case of ablation at another pulse width (200 ns) this effect manifests itself only at higher concentrations (50 and 80 mg L^{-1}).

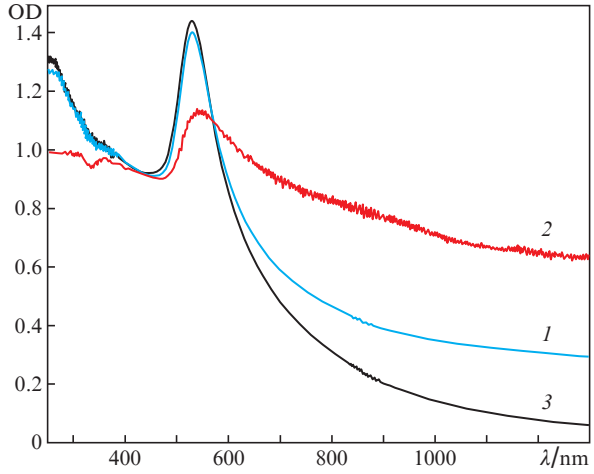

Figure 7. (Colour online) Extinction spectra of colloidal solutions of gold nanoparticles produced as a result of target ablation by Yb:KGW laser radiation in (*1*) water and (*2*, *3*) $MgSO_4$ aqueous solutions with concentrations of (*2*) 1 and (*3*) 5 mg L^{-1}; the fluence is 10 J cm^{-2}, the ablation time is 20 min.

According to the model presented in [25], elongated nanoparticles are formed because of the interaction between the repulsive electrostatic field of nanoparticles and their van der Waals attraction. During laser ablation in liquid, two elongated nanoparticles, each surrounded with divalent ions, undergo repulsion when they are in the orthogonal position (the repulsive electrostatic force dominates) or attraction when they are oriented parallel to each other (the van der Waals attraction dominates). We should note that the experiments with addition of $CaCl_2$ to an aqueous solution of spherical gold nanoparticles in the absence of laser radiation also revealed a red wing (although not much pronounced) in the extinction spectrum. The presence of calcium ions barely affects the position (near 520 nm) of the absorption peak corresponding to the transverse plasmon resonance (Fig. 8).

Under our experimental conditions, the gold nanoparticles formed by ablation of a gold target in water had a negative charge (their ζ-potential during ablation by 200-ns pulses is −45 mV [19]). In the presence of divalent ions (for example, Ca^{2+} or Mg^{2+}) in liquid, the negative charge of a nanoparticle is partially or completely compensated for by the adsorption of

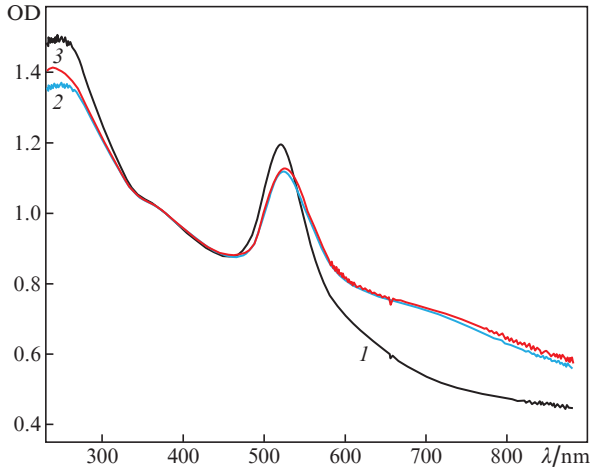

Figure 8. (Colour online) Extinction spectra of colloidal solutions of gold nanoparticles in water (*1*) and after target ablation by ytterbium laser radiation in $CaCl_2$ aqueous solutions with concentrations of (*2*) 10 and (*3*) 50 mg mL^{-1}.

these ions on it. In some concentration range of divalent ions compensation occurs only partially, leading to asymmetric interaction between two particles, which was described in [25]. The ζ-potential of the gold nanoparticles generated during target ablation by 1-ps pulses (Fig. 7) was not measured; however, it is apparently higher than in the case of ablation by 200-ns pulses (Fig. 8) because the transition from elongated to spherical shape of nanoparticles occurs at another concentration of divalent ions.

Thus, the results of this study show that laser ablation of a gold target in aqueous solutions of salts of divalent ions produces elongated nanoparticles with different aspect ratios. An increase in the ablation time for nanosecond laser pulses increases the number of elongated particles. These particles can be applied in laser hyperthermia.

Acknowledgements. We are grateful to the Common Use Centre of the General Physics Institute of the Russian Academy of Sciences and to E. Stratakis and E. Skoulas (IESL FORTH, Greece) for their help in carrying out the experiments.

This work was partially supported by the Russian Foundation for Basic Research (Grant Nos 18- 52-70012_e_Asia_a, 19-02-00061 A, 18-32-01044_mol_a, and 20-32-70112_Stabil'nost'). The study was also supported by the National Research Nuclear University MEPhI within the Russian Academic Excellence Project (Contract No. 02.a03.21.005 on 27 August 2013) and supported by the Presidium of the Russian Academy of Sciences (Programme No. 5 'Photonic Technologies in Probing Inhomogeneous Media and Biological Objects') and partially supported by project NFFA ID 674.

References

1. Amendola V., Pilot R., Frasconi M., Maragò O.M., Iatì M.A. *J. Phys. Condens. Matter*, **29**, 203002 (2017).
2. Shafeev G.A., in *Laser Ablation: Effects and Applications* (New York: Nova Science Publishers, 2011) pp 191–225; doi:10.1201/b11623-8.
3. Itina T.E. *J. Phys. Chem. C*, **115**, 5044 (2011).
4. Riabinina D. et al. *Appl. Phys. A: Mater. Sci. Process.*, **102**, 153 (2011).
5. Danilov P.A. et al. *Laser Phys. Lett.*, **14**, 056001 (2017).
6. Maciulevičius M. et al. *Appl. Phys. A: Mater. Sci. Process.*, **111**, 289 (2013).
7. Saha K., Agasti S.S., Kim C., Li X., Rotello V.M. *Chem. Rev.*, **112**, 2739 (2012).
8. Cho E.S. et al. *Nat. Mater.*, **11**, 978 (2012).
9. Amendola V., Meneghetti M. *J. Mater. Chem.*, **22**, 24501 (2012).
10. Maier S.A. *Plasmonics: Fundamentals and Applications* (Springer, US, 2007); doi:10.1007/0-387-37825-1.
11. Luk'yanchuk B. et al. *Nat. Mater.*, **9**, 707 (2010).
12. Oko D.N. et al. *Electrochim. Acta*, **159**, 174 (2015).
13. Dell'Aglio M. et al. *Appl. Surf. Sci.*, **374**, 297 (2016).
14. Barzan M., Hajiesmaeilbaigi F. *Eur. Phys. J. D*, **70**, 1 (2016).
15. Barmina E.V., Simakin A.V., Shafeev G.A. *Chem. Phys. Lett.*, **678**, 192 (2017).
16. Barmina E.V., Simakin A.V., Shafeev G.A. *Chem. Phys. Lett.*, **655-656**, 35 (2016).
17. Kanitz A. et al. *Plasma Sources Sci. Technol.*, **28**, 103001 (2019).
18. Zhil'nikova M.I., Barmina E.V., Shafeev G.A. *Phys. Wave Phenom.*, **26**, 85 (2018).
19. Zhilnikova M., Barmina E., Shafeev G., Rakov I., in *Gold Nanoparticles: Advances in Research and Applications* (New York: Nova Science Publishers, 2020) pp 63–86.
20. Shafeev G.A. et al. *Appl. Surf. Sci.*, **466**, 477 (2019).
21. Alvarez M.M. et al. *J. Phys. Chem. B*, **101**, 3706 (1997).
22. Creighton J.A., Eadon D.G. *J. Chem. Soc. Faraday Trans.*, **87**, 3881 (1991).
23. Chang S.-S., Shih C.-W., Chen C.-D., Lai W.-C., Wang C.R.C. *Langmuir*, **15**, 701 (1999).
24. Link S., Burda C., Nikoobakht B., El-Sayed M.A. *J. Phys. Chem. B*, **104**, 6152 (2000).
25. Stover R.J. et al. *Langmuir*, **32**, 1127 (2016).